

Enhancement of Cr and Fe diffusion in ZnSe/S laser crystals via annealing in vapors of Zn and hot isostatic pressing

OZARFAR GAFAROV,* ALAN MARTINEZ, VLADIMIR FEDOROV, AND SERGEY MIROV

Center for Optical Sensors and Spectroscopies and the Department of Physics, University of Alabama at Birmingham, CH 310, 1300 University Blvd., Birmingham, AL 35294, USA

*ozarfar@uab.edu

Abstract: Enhancement of the thermal diffusion rates of Cr and Fe in ZnSe/ZnS was studied using two different approaches. Enhancement of Cr diffusion in ZnSe was achieved by application of excess Zn atmosphere during the thermal diffusion of Cr, where ~2.2 times improvement in the diffusion coefficient was seen over the standard diffusion technique. Also, the diffusion coefficient of Fe in ZnSe and ZnS was improved by 13 and 14 times, respectively, when diffusion was done under hot isostatic pressing.

© 2016 Optical Society of America

OCIS codes: (160.6990) Transition-metal-doped materials; (160.3380) Laser materials.

References and links

1. S. Mirov, V. Fedorov, D. Martyshkin, I. Moskalev, M. Mirov, and S. Vasilyev, "Progress in Mid-IR Lasers Based on Cr and Fe Doped II-VI Chalcogenides", *IEEE J. of Selected Topics in QE* **21**(1), 1601719 (2015).
2. I. Moskalev, S. Mirov, M. Mirov, S. Vasilyev, V. Smolski, A. Zakrevskiy, and V. Gapontsev, "140 W Cr:ZnSe laser system," *Opt. Express* **24**(18), 21090–21104 (2016).
3. S. Vasilyev, I. Moskalev, M. Mirov, V. Smolski, S. Mirov, and V. Gapontsev, "Recent breakthroughs in solid-state mid-IR laser technology," *Laser Tech. J.* **13**(4), 1–5 (2016).
4. A. Martinez, L. Williams, V. Fedorov, and S. Mirov, "Gamma radiation-enhanced thermal diffusion of iron ions into II-VI semiconductor crystals," *Opt. Mater. Express* **5**(3), 558–565 (2015).
5. K. Bentley and R. Kawai, University of Alabama at Birmingham, personal, personal communication.
6. U. M. Gosele, "Fast Diffusion in Semiconductors," *Annu. Rev. Mater. Sci.* **18**(1), 257–282 (1988).
7. A. E. Dormidonov, K. N. Firsov, E. M. Gavrishchuk, V. B. Ikonnikov, S. Yu. Kazantsev, I. G. Kononov, T. V. Kotereva, D. V. Savin, and N. A. Timofeeva, "High-efficiency room-temperature ZnSe:Fe²⁺ laser with a high pulsed radiation energy," *Appl. Phys. B* **122**(8), 211 (2016).
8. J.-O. Ndap, K. Chattopadhyay, O. O. Adetunji, D. E. Zelmon, and A. Burger, "Thermal diffusion of Cr²⁺ in bulk ZnSe," *J. Cryst. Growth* **240**(1–2), 176–184 (2002).
9. S. B. Zhang, S.-H. Wei, and A. Zunger, "Intrinsic n-type versus p-type doping asymmetry and the defect physics of ZnO," *Phys. Rev. B* **63**(7), 075205 (2001).
10. L. L. Kulyuk, D. D. Nedeoglo, A. V. Siminel, and K. D. Sushkevich, "Effect of annealing of ZnSe:Cr crystals in Bi(Zn) melt on the intensity of radiation bands of Cr ions," *Moldavian J. of the Physical Sciences* **9**(2), 138–140 (2010).
11. M. Aven and H. H. Woodbury, "Purification of II-VI compounds by solvent extraction," *Appl. Phys. Lett.* **1**(3), 53 (1962).
12. G. H. Blount, A. C. Sanderson, and R. H. Bube, "Effects of Annealing on the Photoelectronic Properties of ZnS Crystals," *J. Appl. Phys.* **38**(11), 4409 (1967).
13. A. V. Savitskii, V. I. Tkachuk, and P. N. Tkachuk, *Sov. Phys. Semicond.* **26**, 536 (1992).
14. E. V. Karaksina, V. B. Ikonnikov, and E. M. Gavrishchuk, "Recrystallization Behavior of ZnS during Hot Isostatic Pressing," *Inorg. Mater.* **43**(5), 452–454 (2007).
15. D. R. Vij and N. Singh, *Luminescence and Related Properties of II-VI Semiconductors* (Nova Science Publishers, 1998), p 172.

1. Introduction

The middle Infrared (mid-IR) 2–20 μm region of the electromagnetic spectrum attracts a lot of interest. It is also called the "molecular fingerprint" region since many organic molecules feature strong and narrow absorption spectra there. The interest in mid-IR lasers arises due to a vast range of applications in material processing, non-invasive medical diagnosis, industrial

process control, environmental monitoring, free space optical communication, and many others.

Transition metal (TM) doped II-VI semiconductors like Fe:ZnSe/S and Cr:ZnSe/S have proven to be the materials of choice for fabrication of mid-IR gain media. Due to tetrahedral orientation, intrashell transitions of the TM ions take place in the mid-IR (${}^5T_2 \leftrightarrow {}^5E$). Other favorable features of the TM:II-VI materials include a four-level energy structure, absence of excited state absorption, close to 100% quantum efficiency of fluorescence (for Cr doped II-VI media), and broad mid-IR vibronic absorption and emission bands. Mid-IR lasers based on Cr^{2+} and Fe^{2+} doped ZnSe/S exhibit operation with a wide range of tunability (1.8–5.2 μm), high output power (>140W), high energy (>2.1J), narrow linewidth (<100 kHz), fs-pulses (<30 fs), and other favorable characteristics [1–3].

Polycrystalline gain elements fabricated by post-growth thermal diffusion of TM impurities in II-VI hosts feature good optical quality and enable superior laser characteristics as compared to single crystals [1]. In spite of the significant progress that has been achieved in post-growth thermal diffusion technology [1] some difficulties associated with diffusion of certain TM ions in certain II-VI hosts still remain unresolved. This results in small diffusion lengths and large concentration gradient of impurity, and limits fabrication of large scale gain elements. One of the methods for improving the diffusion rate is radiation enhanced thermal diffusion process. Using ${}^{60}\text{Co}$ as the gamma irradiation source our group demonstrated a 50% and 25% enhancement in the diffusion length of Fe in ZnS and ZnSe, respectively [4]. Based on computer simulations and theoretical considerations, it is predicted that the presence of interstitial cations may increase the diffusion rate in these crystals [5,6]. This takes place because the energy barrier is lower for an interstitial to kick out a nodal cation into interstitial position, which, in turn, will cause another similar process and mediate the migration of the diffusing ion in the cation sublattice [5]. In our crystals this process should take place in the presence of interstitial Zn. Thus, the effects of excessive Zn, provided by co-annealing in Zn vapor, on diffusion characteristics of Cr in ZnSe were studied.

Another method for enhancement of diffusion is related to the diffusion temperature increase [7]. The use of elevated temperatures is accompanied by a strong sublimation of ZnS and ZnSe and reduction of the crystal's optical quality. The issue may be mitigated by simultaneous application of high temperature and high pressure. Thus, Hot Isostatic Pressing was used as the means for simultaneous application of high temperature (up to 1300° C) and high pressure (up to 3000 atm) to study diffusion processes of Fe in ZnSe and ZnS.

2. Co-annealing in vapor of Zn

Chemical vapor deposition grown polycrystalline samples of ZnSe (3.5x8x7 mm^2) were thoroughly cleaned with acetone, methanol, and DI-water, because surface contamination can create significant barriers for ion diffusion. A 150 nm thick Cr film was deposited on one of the largest facets of the crystal using magnetron sputtering. Samples were placed in quartz tube and a ~0.8g piece of Zn metal was added such that there was no physical contact between the metal and the crystal. Another set of identical crystals was placed in the quartz tubes without the addition of Zn. The second set was used as a reference for comparing the thermal diffusion of Cr with and without co-annealing in vapor of Zn. Quartz tubes were pumped out (10^{-5} Torr) and sealed. Samples were then annealed at 1000° C for 3 days. After annealing samples were removed from quartz tubes. A 1.5mm thick layer was polished-off from the facets normal to the direction of diffusion in order to reduce the surface scattering associated with some surface degradation during the annealing process. The crystals were placed on a translation stage and were scanned across a focused beam of 1560 nm Er: fiber laser in the direction of diffusion. The diameter of the beam was ~80 μm . Figure 1 depicts the experimental setup. Cr^{2+} has an absorption band of the ${}^5T_2 \rightarrow {}^5E$ transition with a peak at 1770nm, the absorption spectra of such transition are shown in Fig. 3. The radiation at

1560nm coincides with this band allowing estimation of the Cr concentration by measuring the power transmitted through the crystal with a thickness $l \sim 4$ mm.

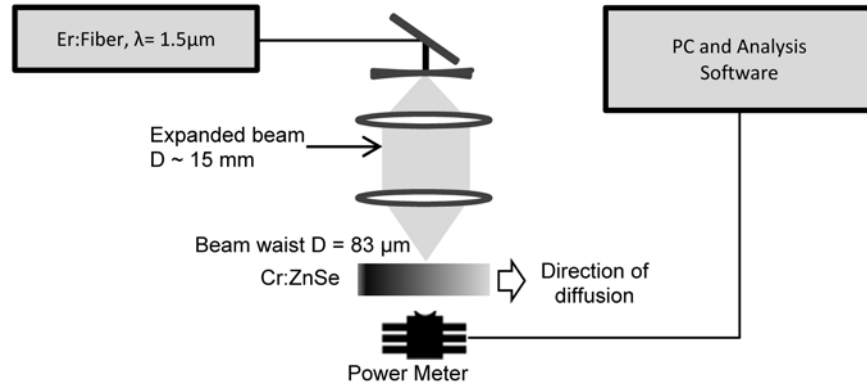


Fig. 1. Experimental setup for measurement of spatial distribution of Cr^{2+} ions.

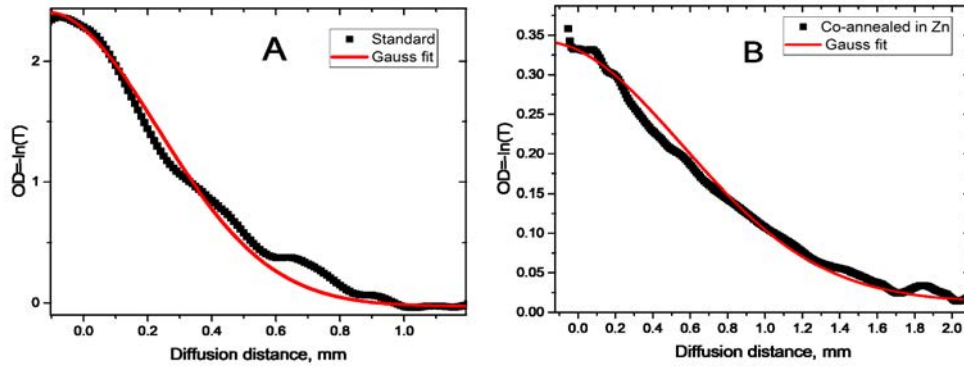


Fig. 2. Optical density as a function of distance from the crystal facet. A) standard thermal diffusion method and B) thermal diffusion in presence of Zn vapor.

Power transmitted through the crystal as a function of diffusion distance was recorded using a power meter connected to PC with analysis software and normalized with respect to the incident power. From the transmission measurements (T) an optical density, $OD = -\ln(T)$, was calculated. Figure 2 shows the plot of OD as a function of distance from the crystal facet (black curve). Due to linear relation between optical density and dopant concentration, the measured dependences were used to calculate the diffusion parameters. Based on Fick's laws of diffusion [8], for a diffuser that spreads into one half-space, the concentration distribution (C) as function of distance and time has a Gaussian form given by Eq. (1).

$$C(x,t) = \frac{M}{\sqrt{\pi Dt}} \exp\left(-\frac{x^2}{4Dt}\right) \quad (1)$$

where M represents the ions diffusing per unit area, D is diffusion coefficient, x and t are distance, and annealing time, respectively. The diffusion length, $L_{\text{diff}} = 2\sqrt{Dt}$, was estimated using parameters from fitting Gaussian curves to the OD plot. Obtained values for the diffusion length were 0.4mm and 0.87mm for the standard and Zn co-annealed diffusion methods, respectively. Hence, an improvement of more than 2.2 times and 4.7 times for diffusion length and coefficient of diffusion of Cr, respectively, was achieved through ZnSe co-annealing in vapor of Zn. Co-annealing in Zn vapor enables an excess of Zn interstitials in the ZnSe lattice [8]. The interstitial Zn^{2+} , which has vibrational energy, kicks out nodal

Cr^{2+}/Zn^{2+} into an interstitial position and occupies the freed nodal position. Then, interstitial Cr^{2+} goes through another cycle of similar nodal-interstitial exchange and propagates further into the crystalline lattice, consequently mediating better diffusion of the desired ions. It is worth noting that, in some instances purification of the crystal from Cr takes place during annealing with Zn. It could result in reduction of chromium concentration in crystals after diffusion or even complete purification when the crystal is in physical contact with the Zn liquid during annealing. This happens due to the fact that the solubility of a solute is usually higher in a liquid solvent than a solid. Similar purification results were seen by other groups in II-VI materials [10–13]. We also found that this effect could be observed when ampoule has a poor vacuum, i.e. oxygen is present in the ampoule. At 1000° C there is selenium atmosphere in the ampoule that can react with the deposited Cr film and form CrSe, followed by reaction (2) and (3) enabling Cr precipitation in non-volatile Cr_2O_3 form.

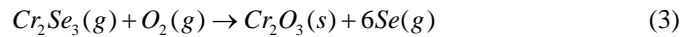
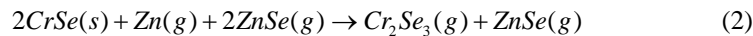


Figure 3 shows the absorption spectra of Cr:ZnSe before and after annealing in vapor of Zn and O_2 as well as in liquid Zn. It can be clearly seen that the characteristic Cr^{2+} absorption due to ${}^5T_2 \rightarrow {}^5E$ transition, with a peak at 1770nm is eliminated, after crystal annealing in Zn vapor in the presence of O_2 , as well as in Zn melt without oxygen. Inductively coupled plasma-mass spectroscopy (ICP-MS), which measures Cr at any valence state, was used to check for possible conversion of Cr^{2+} into any other valence state. After analysis it was seen that Cr concentration that was initially at 90 ppm dropped below the detection limit of 2ppm, confirming effective crystal purification from chromium.

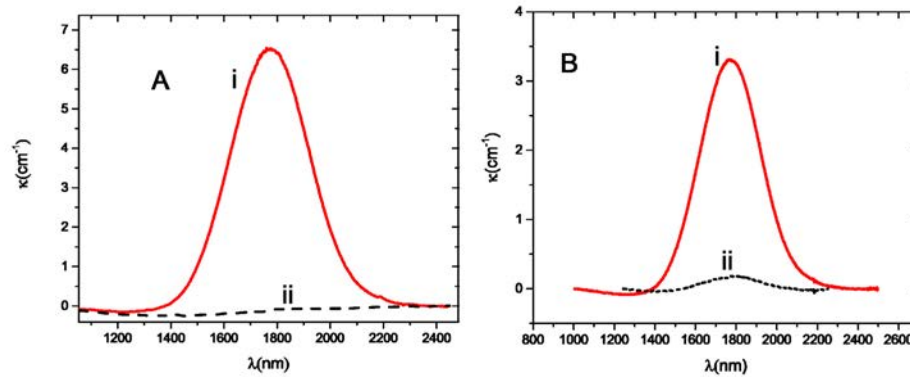


Fig. 3. Absorption coefficient of Cr^{2+} in ZnSe A) before annealing (i), after annealing in vapor of Zn and O_2 (ii), B) before annealing (i), sample after annealing in Zn liquid (ii).

3. Diffusion under hot isostatic pressing

It is well-known that the diffusion rate increases with the increase of temperature. However, utilization of high temperatures is problematic for ZnSe/ZnS, because of the strong sublimation that these crystals have at elevated temperatures. Additionally, ZnS crystals transform from zinc blende (ZB) phase into wurtzite (W) phase at temperature of 1020 °C, which is accompanied by degradation of the optical quality [14]. The problem of sublimation can be addressed by simultaneous application of high pressure during the thermal diffusion process. Hot Isostatic Pressing (HIP) can provide both high temperatures and high pressures, thus HIP was utilized for enhancement of the diffusion rate of Fe in ZnSe/ZnS. CVD grown bulk polycrystals with dimensions $5 \times 5 \times 2 \text{ mm}^2$ were thoroughly cleaned with acetone,

methanol, and DI-water. A 150 nm Fe film was deposited on one of the $5 \times 5 \text{ mm}^2$ facets. The ZnSe and ZnS samples were placed in HIP and treated for 100 hours at 1300°C at two different pressures of 1000 and 3000 atm. Measurement of Fe concentration was carried out in the HIP treated samples using the same platform described in Fig. 1, but instead of the Er:Fiber laser a tunable Cr:ZnS laser operating at 2000 and 2600 nm with a tightly focused beam of $56 \mu\text{m}$ was used. Optical density as a function of diffusion distance was plotted. As can be seen from the Fig. 4 the diffusion length does not depend on the pressure of the HIP chamber and is the same for both pressures. Diffusion coefficient corresponding to the diffusion length of 0.4 mm is $1.1 \times 10^{-9} \text{ cm}^2 / \text{s}$, this is a ~ 14 times improvement over the diffusion coefficient of $8 \times 10^{-11} \text{ cm}^2 / \text{s}$ measured at 950°C [4]. The diffusion length of Fe in ZnSe treated at 1300°C and 3000 atm is 0.84 mm, as can be seen in Fig. 5(a), this translates to a diffusion coefficient of $4.9 \times 10^{-9} \text{ cm}^2 / \text{s}$. This is an improvement of ~ 13 times as compared to diffusion coefficient at 950°C [4].

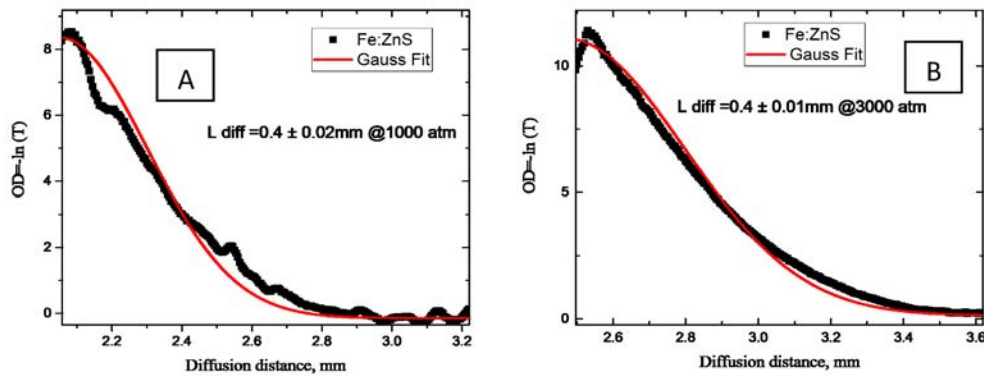


Fig. 4. Optical density as a function of distance from the crystal facet in ZnS annealed at 1300°C , 1000 atm (A) and 3000 atm (B).

A second method was used to measure the Fe concentration using characteristic absorption of Fe^{2+} due to ${}^5E \rightarrow {}^5T_2$ transition. Absorption spectra of the samples shown in Fig. 5(b) were measured with Shimadzu FTIR spectrophotometer at room temperature by consequently polishing-off $\sim 40\text{--}100 \mu\text{m}$ from the surface from which diffusion occurred. Graph of optical density vs polished-off thickness was obtained by normalizing to the value of the maximum optical density.

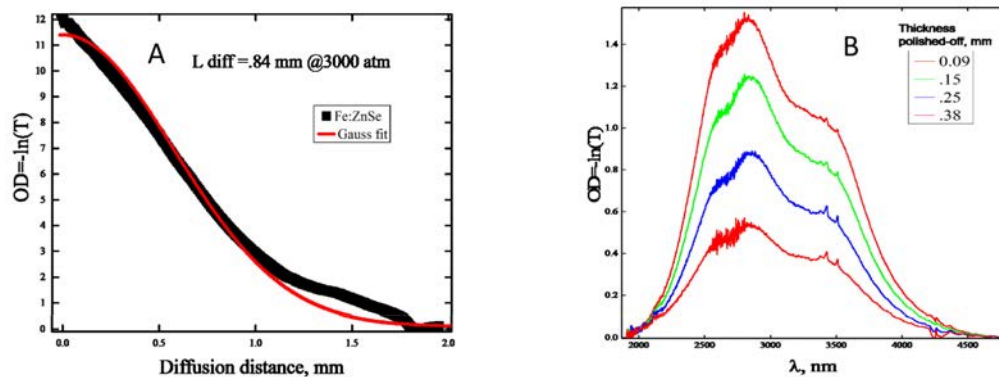


Fig. 5. Optical Density as a function of distance from the crystal facet in ZnSe annealed at 1300°C , and 3000 atm (A). Absorption spectrum of Fe:ZnSe crystal measured in the direction of diffusion after polishing-off (B).

Using the solution of concentration distribution given in Eq. (1) the dependence of the optical density on the polished-off thickness (d) can be defined as,

$$OD(z) = \int_z^{\infty} \sigma C(x,t) dx = \sigma M \left[1 - \operatorname{erf} \left(\frac{z}{4Dt} \right) \right] \quad (4)$$

where σ is the absorption cross-section and the error function is given by Eq. (4).

$$\operatorname{erf}(x) = \frac{2}{\sqrt{\pi}} \int_0^x \exp(-\xi^2) d\xi \quad (5)$$

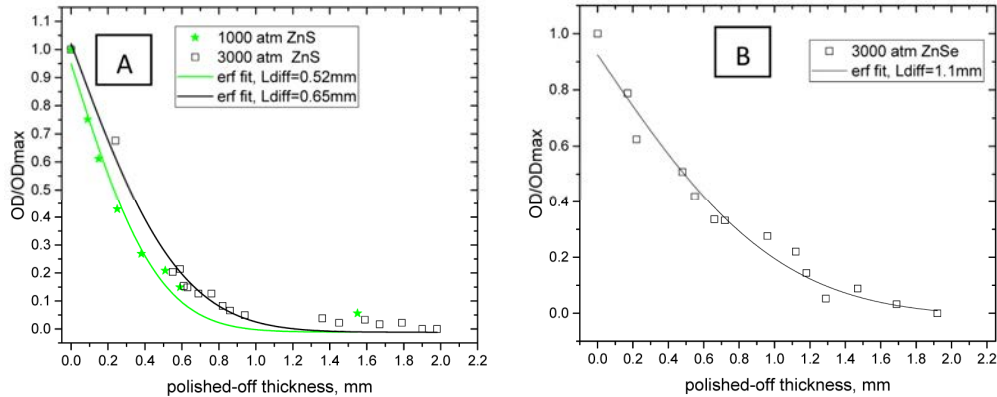


Fig. 6. Normalized optical density as a function of polished-off thickness ZnS (A) and ZnSe (B).

Fitting according to the Eq. (3) was done, as shown by solid lines in Fig. 6. From the parameters of the fit the diffusion length of Fe in ZnS was calculated to be 0.52mm and 0.65mm for 1300° C HIP treatments at 1000 atm and 3000atm, respectively. For Fe diffusion in ZnSe at 1300° C and 3000 atm the diffusion length was calculated to be 1.1mm. These results are in agreement with the more precise laser scanning method. The activation energies of the diffusion processes of Fe in ZnSe and ZnS were calculated using the simple diffusion model given by Eq. (5), and the ratio of diffusion coefficients at two different temperatures of 950° C and 1300° C. Calculated values were 1.22 eV and 1.25 eV for ZnSe and ZnS, which are very similar. It was seen that the grain size grows from ~40μm to ~250μm after HIP treatment of ZnS, similar grain size was reported by other groups as well [15]. On the other hand the grain size grows much faster in ZnSe. The smaller grains size in ZnS creates a much higher grain boundary concentration than in ZnSe. Since diffusion predominantly occurs through the grain boundaries diffusion in ZnS is enhanced to a higher degree.

$$D = D_0 \exp\left(-\frac{E_a}{kT}\right) \quad (6)$$

Here D is the diffusion coefficient, D_0 is the pre-exponential component, E_a is the activation energy, k is the Boltzmann constant and T is the temperature.

X-Ray Diffractometry (XRD) was used to verify the crystallographic phase of the HIP treated ZnS crystals with initial ZB and W structures. The XRD inspection was performed using a 2θ-scan x-ray diffraction (Philips X-Pert MPD, The Netherlands) with a Cu K-alpha anode. Spectra were measured in the 10° to 74° range of 2θ with a step size of 0.05 degrees and accumulation time of 2s. It was found that during preparation of the ZnS powder for XRD measurements the initial W phase of the polycrystalline samples were transformed to ZB by mechanical grinding at room temperature. Therefore, in our analysis only bulk

polycrystalline samples without mechanical grinding were used. Thus, the ratio of the diffraction peak amplitudes could be different in comparison with standard powder pattern.

In our experiments both W and ZB polycrystalline samples were used. The XRD patterns in Fig. 7 show that the used HIP conditions ($P = 1000$ atm, $T = 1300^\circ\text{C}$) cause partial phase transformation from W to ZB and partial of W phase. More importantly it was seen that HIP treatment preserves the ZB crystallographic structure, which is crucial for practical applications.

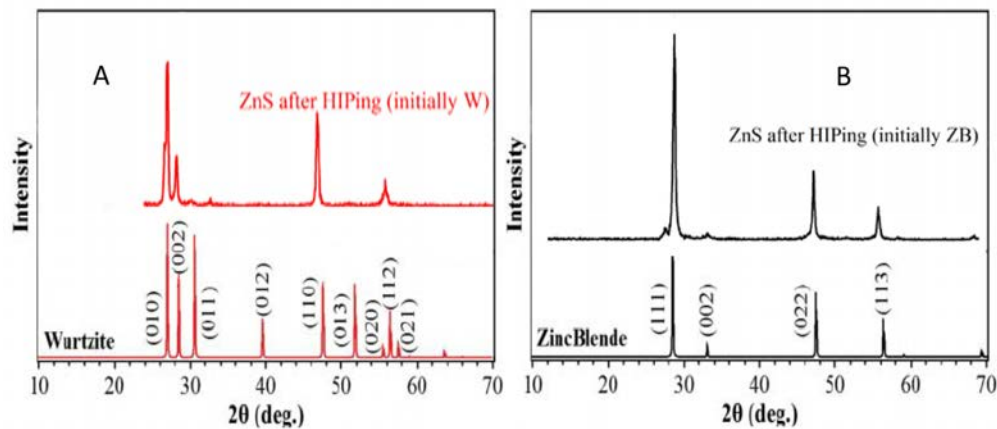


Fig. 7. XRD pattern of HIP treated of predominantly W (top A) and ZB (top B) ZnS. The standard patterns of W and ZB are from JCPDS card 79-2204 and 77-2100, respectively A and B bottom.

4. Conclusion

Two different methods were used to study enhancement of diffusion rate of Cr and Fe in polycrystalline ZnSe and ZnS. The first method was through help of interstitial Zn provided by co-annealing in Zn vapor during the thermal diffusion process. In this experiment diffusion coefficient was improved by ~ 4.7 times as compared to “Standard” diffusion. In the second method HIP was utilized to provide high temperatures and suppress sublimation by high pressure. The diffusion coefficient of Fe was enhanced by 13 times and 14 times in ZnSe and ZnS, respectively, as compared to the standard diffusion at 950°C . The slower growth in diffusion coefficient of Fe in ZnSe can be due to a stronger increase in the grain size of ZnSe with respect to ZnS. Transformation of ZB into W phase in ZnS during its annealing at temperatures in excess of 1020°C is usually accompanied by an increase of scattering and overall degradation of the crystal optical quality. It was demonstrated that HIP treatment at much higher temperatures is capable to suppress transformation of ZB into W phase making it a practically viable method for diffusion enhancement.

Acknowledgments

The authors would like to acknowledge funding support from the AF Office of Scientific Research (Award No. FA9550-13-1-0234). The work reported here partially involves intellectual property developed at the University of Alabama at Birmingham (UAB). This intellectual property has been licensed to the IPG Photonics Corporation. Drs. Fedorov and Mirov declare competing financial interests.